Compressibility Measurements of Quasi-One-Dimensional Quantum Wires

L. W. Smith,[1,*] A. R. Hamilton,[2] K. J. Thomas,[3,†] M. Pepper,[4] I. Farrer,[1] J. P. Griffiths,[1] G. A. C. Jones,[1] and D. A. Ritchie[1]

[1]*Cavendish Laboratory, J. J. Thomson Avenue, Cambridge, CB3 OHE, United Kingdom*
[2]*School of Physics, The University of New South Wales, Sydney 2052, Australia*
[3]*Department of Electronic and Electrical Engineering, Sungkyunkwan University, Suwon 440-746, South Korea*
[4]*Department of Electronic and Electrical Engineering, University College London, London, WC1E 7JE, United Kingdom*
(Received 27 May 2011; published 13 September 2011)

We report measurements of the compressibility of a one-dimensional quantum wire, defined in the upper well of a GaAs/AlGaAs double quantum well heterostructure. A wire defined simultaneously in the lower well probes the ability of the upper wire to screen the electric field from a biased surface gate. The technique is sensitive enough to resolve spin splitting of the subbands in the presence of an in-plane magnetic field. We measure a compressibility signal due to the 0.7 structure and study its evolution with increasing temperature and magnetic field. We see no evidence of the formation of the quasibound state predicted by the Kondo model, instead our data are consistent with theories which predict that the 0.7 structure arises as a result of spontaneous spin polarization.

The conductance of a quasi-one-dimensional (1D) quantum wire [1], quantized in units of $2e^2/h$ [2,3], is in general well described by a noninteracting single-particle picture. However, below the first conductance plateau, a feature close to 0.7 $(2e^2/h)$ exists [4], believed to arise from electron interactions. Many theories have been proposed as to why this "0.7 structure" occurs, including spontaneous spin polarization [4,5], the Kondo effect [6,7], and Wigner crystallization [8,9]. Its cause has yet to be conclusively determined, and this topic remains one of significant interest [4–11].

To date, most experimental studies of 1D systems have focused on measuring conductance through the quantum wire. Notable exceptions include thermopower [12,13] and shot-noise [14,15] measurements, but, like conductance, these are thermodynamically nonequilibrium measurements. We measure the compressibility of a 1D wire, which, as a thermodynamic property, measures the equilibrium properties of the system.

The compressibility (κ) of a two-dimensional electron gas (2DEG) is given by $\kappa^{-1} = N^2 \partial\mu/\partial N$, where μ is the chemical potential and N is the areal density. The compressibility is directly related to the screening ability of the electron gas, such that a highly compressible system more easily screens local electric fields. This can be measured using two closely separated electron layers in a double quantum well (DQW) structure, first shown by Eisenstein *et al.* [16,17]. Compressibility measurements are a useful tool for investigating interaction effects in the fractional quantum Hall regime [16], and have recently been used to study electronic states in graphene [18].

In early compressibility studies of 1D systems, arrays of quantum wires were investigated using capacitive techniques [19,20]. Later, Castleton *et al.* [21] measured an individual quantum wire, which showed enhanced compressibility as each 1D subband was populated. More recently, Lüscher *et al.* [22] predicted a compressibility feature associated with the formation of a quasibound state in the 1D channel, using density functional theory (DFT) calculations.

In this Letter we present measurements of the compressibility of a 1D wire in zero and finite in-plane magnetic field. We resolve the spin splitting of 1D subbands in the compressibility signal, due to the high sensitivity of our technique. As the magnetic field is increased, the compressibility signal shows a peak associated with the lowest spin-split subband. A very similar peak related to the 0.7 structure emerges as a function of temperature at zero field. Our results support earlier studies which suggest that the origin of the 0.7 structure is related to spontaneous spin polarization [4]. We do not observe the features predicted in Ref. [22] for a Kondo-like origin of the 0.7 structure, despite the sensitivity of our measurement.

Our samples were fabricated on DQW GaAs/AlGaAs heterostructures, in which two 15 nm-wide quantum wells are separated by a 30 nm AlGaAs barrier. The center of the quantum wells are 292.5 and 337.5 nm below the surface of the wafer. Split-gate devices with a midline gate were patterned using electron-beam lithography, as shown schematically in Fig. 1(b). The split gates were 0.5 μm long and 0.8 μm wide, and the midline gate was 0.3 μm wide, positioned at the center of the split gate. The combination of split and midline gates allows 1D channels to be defined in both layers simultaneously [21]. Applying a voltage on the bar gate [see Fig. 1(b)] depletes electrons from the top layer, allowing the lower layer to be independently contacted. Figure 1(a) shows the successive depletion of the upper and lower 2D layers as a function of bar-gate voltage (V_{bar}), marked by (u) and (l), respectively. When $V_{bar} = 0$ we measure the conductance of both layers (G_{12}), and for
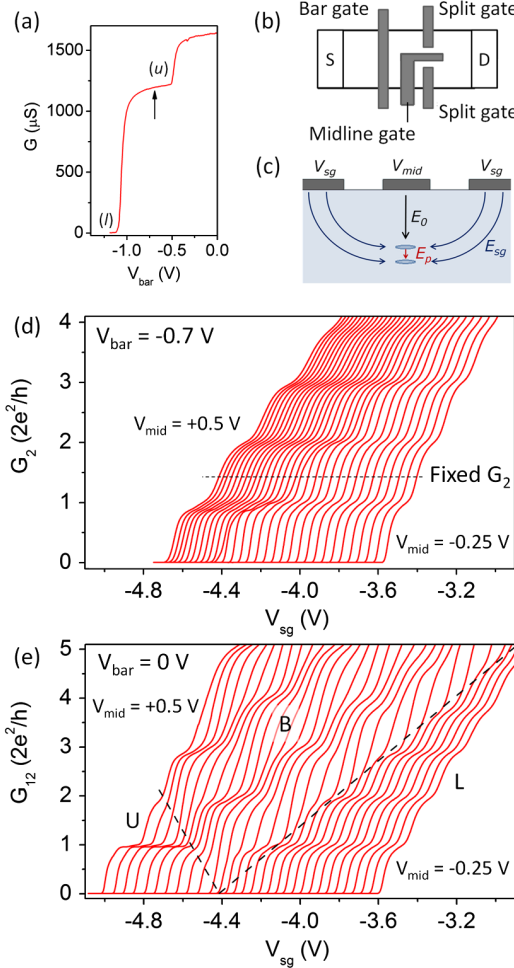
FIG. 1 (color online). (a) Conductance as a function of V_{bar}.
Labels (u) and (l) mark the depletion of the upper and lower
electron layers, respectively. The arrow indicates $V_{bar} =
-0.7$ V, typically applied to fully deplete the upper layer.
(b) Device schematic, showing the bar gate, split gates, and
midline gate. The source and drain Ohmic contacts are marked
by S and D, respectively. (c) Simplified diagram of a cross
section through the device, showing the electric fields generated
by biasing the split gates (E_{sg}), the midline gate (E_0), and the
field which penetrates the upper wire (E_p). (d) Conductance
measured through the lower wire alone (G_2) as a function of V_{sg}
($V_{bar} = -0.7$ V). The horizontal dashed line indicates a fixed
G_2. (e) Conductance through both wires (G_{12}) as a function of
V_{sg} ($V_{bar} = 0$ V). In both (d) and (e) V_{mid} is stepped from 0.5 V
on the left to -0.25 V on the right, in 25 mV intervals. Data are
from a typical device, measured at 300 mK, and corrected for
series resistance.

$V_{bar} = -0.7$ V (marked by the arrow), we measure the
conductance of the lower layer alone (G_2).

Crucial to this experiment is the quality of devices and
stability of the 2DEG. Over 20 devices were tested at
300 mK. Devices which exhibited clean, stable, and
reproducible conductance characteristics were selected
for further measurement. The data presented in Figs. 2–4
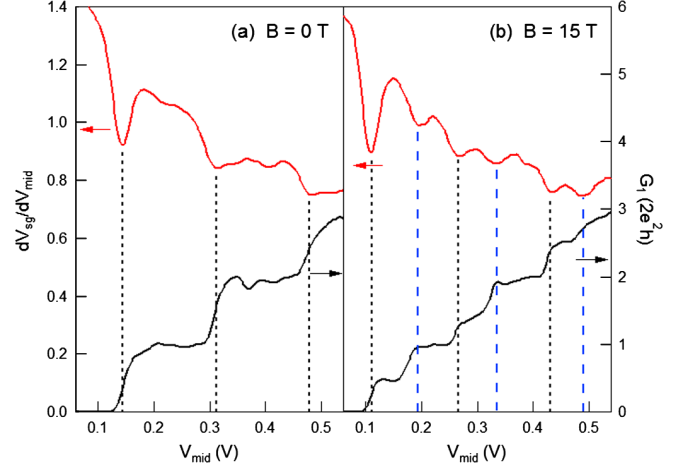are from a device for which the total carrier density

FIG. 2 (color online). (a) Compressibility signal dV_{sg}/dV_{mid}
against V_{mid} [gray (red) trace, left axis], for $G_2 \approx 1.5(2e^2/h)$
($B = 0$ T). The conductance of the upper wire (G_1) is plotted in
black (right axis). Minima in dV_{sg}/dV_{mid} coincide with inter-
plateau rising edges, as illustrated by the dashed lines. The
equivalent data at $B = 15$ T are shown in (b) for $G_2 \approx
1.75(2e^2/h)$. The lifting of the spin degeneracy results in the
appearance of spin-split plateaus in G_1, and we resolve addi-
tional minima in dV_{sg}/dV_{mid} associated with the spin splitting of
subbands (marked by the long-dashed lines). This measurement
was performed at 25 mK.

and mobility were measured to be 2.4×10^{11} cm^{-2} and
3×10^6 cm^2 V^{-1} s^{-1}, respectively (all measurements were
performed in the absence of illumination). We measured
similar results in two further devices. Data presented were
measured using a dilution refrigerator with a base tempera-
ture of 25 mK and a ^{3}He system at 300 mK. A magnetic
field was applied in the plane of the 2DEG, perpendicular
to the transport direction.

Figure 1(d) shows the conductance of the lower wire
(G_2) as a function of V_{sg}. The bar gate is biased so that
current only flows through the lower wire, even if the upper
wire is occupied. For each trace V_{mid} is fixed, and between
traces V_{mid} is stepped by 25 mV, from 0.5 V on the left to
-0.25 V on the right. When the bar-gate bias is removed,
the total conductance (G_{12}) is measured, shown in
Fig. 1(e). Regions are identified in which either the upper
wire alone is populated (U), both wires are populated
simultaneously (B), or the lower wire alone is populated
(L) [21]. The dashed lines mark a "V" separating these
regions. On the left and right of the V conductance is
quantized in $2e^2/h$ multiples, indicating single-wire trans-
port. Conductance in the middle region is quantized in
$4e^2/h$ multiples, due to transport through the two wires
in parallel. The upper-wire conductance (G_1) can be ex-
tracted from these data, since $G_1 = G_{12} - G_2$. We do not
observe coupling between the two wires, as seen in devices
with more closely spaced quantum wells [23].

To determine the compressibility of the upper 1D wire,
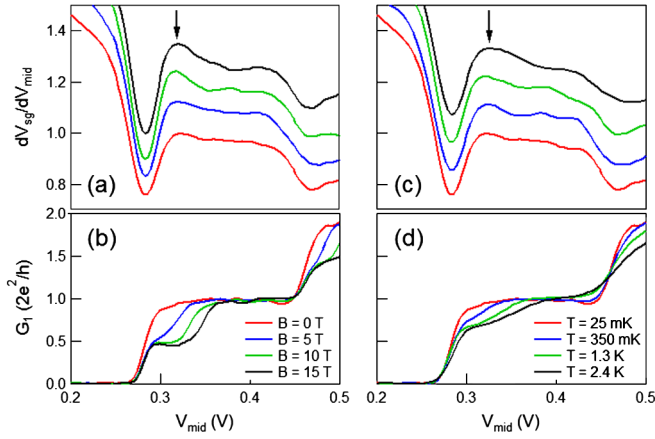we measure how well it screens the electric field from the

FIG. 3 (color online). (a),(b) Magnetic-field dependence of dV_{sg}/dV_{mid} and corresponding G_1, respectively, for $B = 0$, 5, 10, and 15 T. $B = 15$ T data are shifted horizontally by 6.5 mV to align with other data. Measurements were performed at $T = 25$ mK. In (b) data are vertically offset for clarity; the arrow marks the peak which develops as B increases. (c), (d) Temperature dependence of dV_{sg}/dV_{mid} and corresponding G_1, respectively, at $T = 25$ mK, 350 mK, 1.3 K, and 2.4 K. $T = 350$ mK, 1.3 K, and 2.4 K data are shifted horizontally by 2.5, 5, and -3.5 mV, respectively, to align with 25 mK data [26]. In (c) dV_{sg}/dV_{mid} are vertically offset for clarity; the peak which develops with increasing temperature is marked by the arrow. Temperature-dependent measurements were performed at $B = 0$ T. $G_2 = 0.23(2e^2/h)$ for both data sets [29].
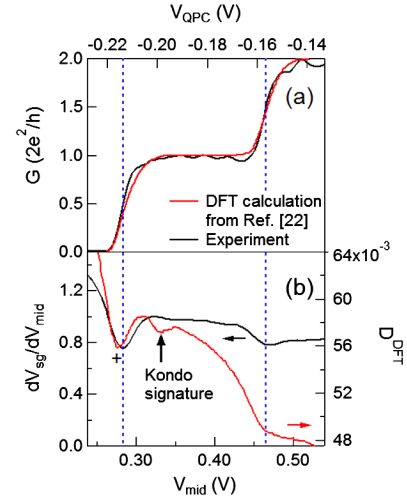

FIG. 4 (color online). (a) Calculated conductance of the quantum point contact (QPC) from Lüscher *et al.* [22] (red traces, top axis), compared with G_1 at $B = 0$ T and $T = 25$ mK (black trace, bottom axis). Horizontal axes are scaled to align the conductance data. (b) Corresponding derivatives D^{DFT} (from Ref. [22], red trace, right and top axes) and dV_{sg}/dV_{mid} (experimental data, black trace, left and bottom axes). The two y axes are equivalent [27], and are scaled such that the depth of the first minima, marked by +, is of the same magnitude. The secondary dip in D^{DFT}, marked by the vertical arrow, was predicted to be a signature of the formation of a quasibound state. The vertical dashed lines mark transitions between the plateaus as 1D subbands are populated.

midline gate. This is accomplished by changing the electric field incident upon the upper wire (δE_0) from the midline gate, and measuring the corresponding change in the electric field (δE_p) which reaches the lower wire. The electric fields generated by biasing the surface gates are shown in the schematic cross section of the device in Fig. 1(c). The δE_p causes a change in the carrier density, and hence conductance G_2, of the lower wire. This can be compensated for by adjusting V_{sg} by δV_{sg}, so that the total electric field incident on the lower wire remains fixed (thereby keeping G_2 at a constant value [24]). Since δE_p depends on the screening ability of the upper wire, the compressibility is directly related to the measured dV_{sg}/dV_{mid}. For example, if the top wire is highly compressible, V_{mid} is well screened, and little field penetrates onto the lower wire: G_2 changes by a small amount in response to V_{mid}, and dV_{sg}/dV_{mid} is also small. Therefore, minima in dV_{sg}/dV_{mid} correspond to enhanced compressibility. We ignore the direct capacitive coupling between the midline gate and the lower 1D channel, which adds a rising background to the measured signal as V_{mid} decreases.

Figure 2(a) shows the compressibility signal dV_{sg}/dV_{mid} (left axis) and the corresponding conductance of the upper layer G_1 (right axis), at $B = 0$ T. The dV_{sg}/dV_{mid} trace is extracted from data similar to Fig. 1(d), where δV_{sg} is the spacing between neighboring traces at fixed G_2 [shown by

the horizontal dashed line in Fig. 1(d)], and δV_{mid} is the amount that V_{mid} is stepped between traces. In Fig. 2(a) we observe minima in dV_{sg}/dV_{mid} which coincide with the population of 1D subbands in the upper wire. This is highlighted by the vertical dashed lines, which align with transitions (risers) between plateaus in G_1. At these minima V_{mid} is screened most effectively by the upper wire, and therefore the compressibility is maximum. This occurs when the density of states is large (i.e., at the subband edges). This measurement was performed at 25 mK, for $G_2 \approx 1.5(2e^2/h)$ [25].

Figure 2(b) shows the same measurement at $B = 15$ T. Additional plateaus in G_1 confirm that the 1D subbands are spin split, due to the Zeeman energy. Secondary minima appear in dV_{sg}/dV_{mid}, which align with the beginning of spin-split plateaus in G_1 (indicated by the long-dashed lines). The ability to resolve spin splitting in the compressibility signal highlights the sensitivity of our technique, since the Zeeman energy is small ($\approx 10\%$ of the 1D subband spacing). It is interesting to note that at $B = 0$ T the minima in dV_{sg}/dV_{mid} align with the center of risers in G_1, whereas at $B = 15$ T, the additional minima in dV_{sg}/dV_{mid} due to the spin splitting occur at higher energies (larger V_{mid}, tending to align with the beginning of plateaus).

We focus on the magnetic-field dependent behavior of the lowest subband. Figure 3(a) shows the compressibility signal dV_{sg}/dV_{mid} at $B = 0$, 5, 10, and 15 T (vertically offset for clarity); corresponding G_1 traces are given in Fig. 3(b). Significantly, a peak emerges in the compressibility signal as B increases, marked by the arrow in Fig. 3(a). In additional experiments, we observed a clear peak as low as $B = 2$ T. This peak increased smoothly in height and width with increasing B, and coincided in gate voltage with the 0.7 structure as it evolved from $G_1 = 0.7$ to $0.5 \times (2e^2/h)$.

The peak is clearly related to the onset of spin polarization, as it develops in line with the $0.5(2e^2/h)$ plateau in G_1. It represents a reduction in the density of states, which is consistent with the fact that at high fields only the lowest spin subband is populated initially (instead of two spin-degenerate subbands in the zero-field case).

We now examine the temperature dependence of the compressibility. Figure 3(c) shows the compressibility signal dV_{sg}/dV_{mid} at $T = 25$ mK, 350 mK, 1.3 K, and 2.4 K, for $B = 0$ T (vertically offset for clarity). Corresponding G_1 traces are given in Fig. 3(d), and data are horizontally aligned by no more than 5 mV [26]. In Fig. 3(c), a peak in the compressibility signal emerges as temperature increases (marked by the arrow). At the same time a 0.7 structure develops in G_1 [4]. The compressibility response as temperature increases is strikingly similar to the compressibility response as magnetic field is increased at $T = 25$ mK—data in Figs. 3(a) and 3(c) and are almost identical.

We note that while the compressibility data in Figs. 3(a) and 3(c) are so similar, the conductance data in Figs. 3(b) and 3(d) are markedly different. This gives us confidence that we are performing a true thermodynamic measurement; dV_{sg}/dV_{mid} is not simply reflecting changes in G_1, but is rather measuring the density of states in the wire.

We now consider how the compressibility data fit with a Kondo-like scenario, by comparing our results with DFT calculations [27] performed by Lüscher *et al.* [22]. Figures 4(a) and 4(b) show our data at $B = 0$ T and $T = 25$ mK (black traces) with the simulations from Ref. [22] (red traces). We aligned the horizontal axes of our measured data with the simulations from Ref. [22] so that the conductance traces overlapped, as shown in Fig. 4(a). Vertical axes in Fig. 4(b) were aligned such that the depth of the first minima (marked by +) was equal for the experimental and simulated data, to allow an approximate comparison of our data with the only theoretical calculations currently available.

The DFT calculations predict that the formation of the quasibound state necessary for the Kondo effect is signaled by a characteristic dip in the compressibility signal, marked by the vertical arrow in Fig. 4(b). Our experimental data are more sensitive than the simulated response, indicated by better defined minima in our compressibility

signal when a subband in the upper wire is populated. Despite this, we do not observe the secondary dip that was predicted to be the signature of a quasibound state. Therefore, our results do not appear to support a Kondo-like scenario [28].

In contrast to the Kondo model, it has been proposed that the 0.7 structure occurs due to spontaneous spin polarization. This conclusion is primarily motivated by the continuous evolution of the 0.7 structure into the e^2/h plateau as magnetic field increases [4]. In the current experiment, we measure the compressibility response of the 0.7 structure by increasing the temperature, and find that its compressibility response is very similar to that as magnetic field is increased. Indeed, the integrated area under the peak in dV_{sg}/dV_{mid} changes by less than 3% between $T = 2.4$ K, $B = 0$ T [Fig. 3(c)] and $T = 25$ mK, $B = 15$ T [Fig. 3(a)]. One scenario might be that there is a T-dependent increase of the spin gap due to the exchange interaction, which attempts to prevent electrons from entering the spin-up subband. This would cause the compressibility response to be the same for increasing B (which opens the spin gap) and increasing T.

In summary, we have performed compressibility measurements on a 1D quantum wire at zero and finite magnetic fields. We resolve spin splitting in the compressibility signal, which, for the lowest subband, is manifest as a peak in dV_{sg}/dV_{mid} emerging with increasing field. The temperature response in this regime is remarkably similar, suggesting that the origin of the 0.7 structure is due to spin polarization. We compare our data to the Kondo scenario, which does not appear to reproduce our results.

*lws22@cam.ac.uk
†kalarikad@skku.edu

[1] T. J. Thornton, M. Pepper, H. Ahmed, D. Andrews, and G. J. Davies, Phys. Rev. Lett. **56**, 1198 (1986).
[2] D. A. Wharam *et al.*, J. Phys. C **21**, L209 (1988).
[3] B. J. van Wees *et al.*, Phys. Rev. Lett. **60**, 848 (1988).
[4] K. J. Thomas *et al.*, Phys. Rev. Lett. **77**, 135 (1996).
[5] C.-K. Wang and K.-F. Berggren, Phys. Rev. B **54**, R14 257 (1996).
[6] S. M. Cronenwett *et al.*, Phys. Rev. Lett. **88**, 226805 (2002).
[7] Y. Meir, K. Hirose, and N. S. Wingreen, Phys. Rev. Lett. **89**, 196802 (2002).

[8] A. D. Klironomos, J. S. Meyer, and K. A. Matveev, Europhys. Lett. **74**, 679 (2006).

[9] K. A. Matveev, Phys. Rev. Lett. **92**, 106801 (2004).

[10] D. J. Reilly *et al.*, Phys. Rev. Lett. **89**, 246801 (2002).

[11] J. P. Bird, and Y. Ochiai, Science **303**, 1621 (2004).

[12] N. J. Appleyard *et al.*, Phys. Rev. B **62**, R16 275 (2000).

[13] L. W. Molenkamp, H. van Houten, C. W. J. Beenakker, R. Eppenga, and C. T. Foxon, Phys. Rev. Lett. **65**, 1052 (1990).

[14] M. Reznikov, M. Heiblum, H. Shtrikman, and D. Mahalu, Phys. Rev. Lett. **75**, 3340 (1995).

[15] P. Roche *et al.*, Phys. Rev. Lett. **93**, 116602 (2004).

[16] J. P. Eisenstein, L. N. Pfeiffer, and K. W. West, Phys. Rev. Lett. **68**, 674 (1992).

[17] J. P. Eisenstein, L. N. Pfeiffer, and K. W. West, Phys. Rev. B **50**, 1760 (1994).

[18] J. Martin *et al.*, Nature Phys. **4**, 144 (2008).

[19] H. Drexler *et al.*, Phys. Rev. B **49**, 14 074 (1994).

[20] T. P. Smith III *et al.*, Phys. Rev. Lett. **59**, 2802 (1987).

[21] I. M. Castleton *et al.*, Physica (Amsterdam) **249–251B**, 157 (1998).

[22] S. Lüscher *et al.*, Phys. Rev. Lett. **98**, 196805 (2007).

[23] K. J. Thomas *et al.*, Phys. Rev. B **59**, 12 252 (1999).

[24] We choose G_2 to be in a region of high transconductance (i.e., on a riser between plateaus), so that δE_p is amplified by large changes in G_2.

[25] The sensitivity of the measurement is higher for low G_2 [21]. Therefore, data are presented for G_2 at $1.5(2e^2/h)$.

[26] To aid comparison, traces in Figs. 3(c) and 3(d) were horizontally shifted to correct for a small drift in the pinch-off voltage, since measurements were performed over a 2 week period.

[27] In Ref. [22], local spin density approximations were used to model the compressibility response of a quasibound state in the wire, necessary for the Kondo effect. The screened potential ($V_{\det 2}$) from biased surface gates (V_{QPC}) is detected 200 nm below the 2DEG, and the derivative $D^{DFT} \equiv dV_{\det 2}/dV_{QPC}$ is equivalent to our dV_{sg}/dV_{mid} measurement.

[28] We have also compared our measured data at $T = 2.4$ K with the DFT ($T = 0$) calculations. At $T = 2.4$ K there is a strong 0.7 structure in the conductance and an associated peak in the compressibility signal. However, this compressibility feature is qualitatively different from that predicted as a result of the Kondo effect.

[29] $G_2 = 0.23(2e^2/h)$ was chosen because below e^2/h the gradient of the conductance does not change significantly with magnetic field or temperature. Therefore the measurement sensitivity remains constant for all data.